Neuro-Oncology

Neuro-Oncology 17(6), 822–831, 2015
doi:10.1093/neuonc/nou310
Advance Access date 12 November 2014

Druggable targets in pediatric neurocutaneous melanocytosis: Molecular and drug sensitivity studies in xenograft and ex vivo tumor cell culture to identify agents for therapy

Yibing Ruan, Anna Kovalchuk, Aarthi Jayanthan, Xueqing Lun, Yoji Nagashima, Olga Kovalchuk, James R. Wright Jr., Alfredo Pinto, Adam Kirton, Ronald Anderson, and Aru Narendran

Division of Pediatric Oncology, Alberta Children's Hospital and POETIC Laboratory for Preclinical and Drug Discovery Studies, University of Calgary, Calgary, Alberta, Canada (Y.R., A.J., X.L., R.A., A.N.); Department of Biological Sciences, University of Lethbridge, Lethbridge, Canada (A.K., O.K.); Department of Pathology, Yokohama City University School of Medicine and Division of Diagnostic Pathology, Tokyo Women's Medical University Hospital, Tokyo, Japan (Y.N.); Department of Pathology and Laboratory Medicine, Alberta Children's Hospital and Calgary Laboratory Services, Calgary, Canada (J.R.W., A.P.); Department of Neurology, Alberta Children's Hospital, Calgary, Canada (A.K.)

Corresponding Author: Aru Narendran, MD, PhD, Division of Pediatric Oncology, Alberta Children's Hospital, 2888 Shaganappi Trail NW, Calgary, Alberta, Canada T3B 6A8 (a.narendran@ucalgary.ca).

Background. Neurocutaneous melanocytosis (NCM) is a rare congenital disorder that presents with pigmented cell lesions of the brain or leptomeninges in children with large or multiple congenital melanocytic nevi. Although the exact pathological processes involved are currently unclear, NCM appears to arise from an abnormal development of melanoblasts or melanocyte precursors. Currently, it has an extremely poor prognosis due to rapid disease progression and lack of effective treatment modalities.

Methods. In this study, we report on an experimental approach to examining NCM cells by establishing subcutaneous tumors in nude mice, which can be further expanded for conducting molecular and drug sensitivity experiments.

Results. Analysis of the NRAS gene-coding sequences of an established NCM cell line (YP-MEL) and NCM patient cells revealed heterogeneity in NRAS Q61K that activated mutation and possibly consequential differential sensitivity to MEK inhibition. Gene expression studies were performed to compare the molecular profiles of NCM cells with normal skin fibroblasts. In vitro cytotoxicity screens of libraries of targeted small-molecule inhibitors revealed prospective agents for further evaluation.

Conclusions. Our studies provide an experimental platform for the generation of NCM cells for preclinical studies and the production of molecular and in vitro data with which to identify druggable targets for the treatment.

Keywords: molecular profiling, neurocutaneous melanocytosis, targeted therapy.

Biologically, melanomas signify malignant changes in melanocytes that develop predominantly in the skin but can occasionally arise in other organs including the central nervous system (CNS). Neurocutaneous melanocytosis (NCM) is a rare pediatric neoplasm characterized by the presence of large or numerous congenital melanocytic nevi (LCMN) and the benign or malignant growth of melanocytes in the CNS.[1,2] NCM is thought to arise during embryonic neuroectodermal development, during which the migration and proliferation of melanoblasts into the CNS is dysregulated.[2,3] The neurological symptoms of NCM present at 2 peak age groups: infancy and the second or third decade of life.[2,4] The occurrence of symptomatic NCM is very rare but has an extremely poor prognosis. Death occurs within 2 to 3 years of diagnosis.[1,2] It is estimated that up to 25% of patients with LCMN have asymptomatic melanosis.[4] However, ~11.4% of patients with LCMN exhibit NCM,[5] and only 8% survive the disease.[2,5] Additionally, the development of primary brain melanomas in these patients is common.[4] Therapeutic options for patients with NCM are limited to case studies, and there is little experimental evidence to suggest an effective targeted treatment regimen. In general, most case studies on symptomatic NCM do not describe any treatment protocols because of the rapid progress of the disease. Although symptomatic control can be achieved with supportive care, antiseizure medication,

Received 30 July 2014; accepted 5 October 2014

ventriculoperitoneal shunt, or surgical removal of mass lesions, long-term stabilization is rarely achieved in NCM patients with disease activity.[4] Other therapeutic options, such as chemotherapy or radiation, have not significantly altered the outcome of NCM.[1] Therefore, there is an urgent need to establish and validate experimental models to identify functionally relevant druggable targets for the development of effective management strategies for these patients.

Although the exact pathogenesis of NCM is not entirely clear, it appears to originate during the development of the neural crest, with abnormally regulated melanoblast migration and proliferation into the CNS.[4,5] In the majority of cases, affected individuals exhibit melanosis of the meninges with cranial and spinal involvement. Recently, attempts were made to elucidate the genetic alterations found in NCM and LCMN. In a recent study, somatic missense mutations in codon 61 of NRAS (Q61K or Q61R) were found in 80% of the NCM specimens.[6] This mutation activates the Ras/Raf/MEK/MAPK pathway and has been frequently reported in melanoma.[7] More recently, Charbel et al carried out unbiased whole-exome sequencing using matched LCMN samples and concluded that NRAS mutation was the only recurrent genetic event in these patients.[8]

Owing to the rare incidence of NCM, there is a current paucity of accessible primary tumor specimens and functional cell lines with which to study NCM in preclinical programs. YP-MEL is one of the few available NCM cell lines for laboratory studies.[9] It was originally established from the cerebrospinal fluid of a male child with cerebral melanoma and meningeal spread by one of the authors of this report (YN).[9] YP-MEL cells are capable of sustaining growth in a serum-free medium and have a propensity for forming melanocytic tumors in nude mice and inducing melanogenesis in the presence of fetal calf serum in vitro. Here, we report on the growth and expansion of tumor cells obtained from a pediatric patient with leptomeningeal melanocytosis. These cells were then used to identify gene expression profiles in order to provide information on potential growth regulatory pathways and determine sensitivity to therapeutics in vitro.

Materials and Methods

Reagents and Antibodies

Anticancer agents used in this study include IGF-IR inhibitors OSI-906, BMS-754807, and AEW-541; PI3K and mTOR inhibitors PP242, INK128, rapamycin, PF-04691502, GDC-0980, and PIK-75; and Mek inhibitors PD-0325901, RDEA119, AZD-6244, ARRY-162, GSK1120212, and AS703026. These inhibitors were synthesized, checked for purity, and supplied by Chemietek. Antibodies used in this study included anti-phospho-IGF-IR (Tyr1165/66) (Santa Cruz Biotechnology), anti-pAKT (Ser473) (Santa Cruz Biotechnology), anti-AKT (Santa Cruz Biotechnology), anti-IGF-IR (R&D Systems), anti-phospho-ERK1/2 (Thr202/Tyr204) (Cell Signaling), anti-ERK1/2 (Cell Signaling), anti-phospho-mTOR (Ser2248) (Cell Signaling), anti-mTOR (Cell Signaling), and anti-β-actin (Sigma).

Cell Lines

YP-MEL cells were established by Dr. Yoji Nagashima and provided by the Yokohama City University in Japan. These cells were maintained in minimum essential medium (MEM) supplemented with 5% fetal bovine serum (FBS). Brain metastatic malignant melanoma cells were purchased from the Wistar Institute (Cat# WC00090). Normal skin fibroblasts were provided by the molecular genetics services laboratory at Alberta Children's Hospital. The atypical-teratoid rhabdoid tumor (ATRT) cell line BT12 was kindly provided by Dr. Peter Houghton of Nationwide Children's Hospital in Columbus, Ohio.

Patient Cells

The patient was a 2-year-old male with multiple, large congenital nevi who initially presented with increased intracranial pressure, probable seizures, hydrocephalus, Dandy-Walker variant, and classic meningeal enhancement. MRI scanning showed rapid progression of disease over <4 weeks to essential encasement of the entire spine and intramedullary lesions throughout. No biopsy was done. There was a marked initial improvement of his clinical symptoms with dexamethasone. Initial treatment included cyclophosphamide, temozolomide, and sorafenib. Relapse occurred after 6 months, and the child died of progressive disease. Autopsy was performed soon after death following informed consent from the parents (REB approval # 21239), and tumor specimens collected by the pathologist were transferred to culture medium without delay. Tumor was identified visually, and specimens were taken from the posterior fossa region and the spinal cord following confirmation by on-site frozen section. Single-cell suspension of the tumor was prepared by gentle dissociation and filtering through nylon screen. After mouse xenografting, the tumor cells were expanded and cultured in MEM supplemented with 5% FBS (Life Technologies).

Animal Experiments

All xenograft studies were carried out in accordance with the Guide to the Care and Use of Experimental Animals (published by the Canadian Council on Animal Care) and the Guide for the Care and Use of Laboratory Animals (issued by the US National Institutes of Health). All applications were approved by the Animal Care Committee of the University of Calgary (approval permit #M10071). CD-1 nude mice (female, 6–8 weeks old) were purchased from Charles River Canada and housed in groups of 3–5 in a vivarium maintained on a 12-hour light/dark schedule with a temperature of $22 \pm 1^{\circ}$C and a relative humidity of $50\% \pm 5\%$. Food and water were available ad libitum. For the studies described, $\sim 5 \times 10^5$ NCM cells were injected subcutaneously into the hind flank. Visible tumors were photographed in $\sim$3–5 weeks after injection. Palpable tumors were removed $\sim$5 weeks from inoculation under sterile conditions, and single cells suspensions were made and expanded in culture for further studies.

Sanger Sequencing

Sanger sequencing of the NRAS gene in YP-MEL and NCM patient cells was carried out at the DNA core facility of the University of Calgary, using standard automated sequencing methods on a 3730xl Applied Biosystems Genetic Analyzer. The primers used for sequencing were 5′CCAACATTTTTCCCGGCTGT3′ and

5′AGTG
CAGCTTGAAAGTGGCT3′.

Molecular Profiling by Gene Expression Microarray

The gene expression of samples was measured using Illumina's HumanHT-12 v4 BeadChip microarrays with scanning performed using the iScan instrument (Illumina). RNA was extracted from each sample using RNeasy Mini Kit (Qiagen) according to the manufacturer's directions. For the patient NCM cells, single-cell suspensions from tumors were cultured at ∼4 passages in vitro and used for RNA preparation. Five micrograms of RNA was then reverse-transcribed using oligo(dT) primers and Superscript II reverse transcriptase (Life Technologies), followed by labeling and hybridization.

Data Analysis

The scanned microarray data were background-corrected, normalized, and filtered to eliminate genes not expressed in any samples using Illumina's GenomeStudio. The data were then exported to Partek Genomics Suite for further analysis. Differences between YP-MEL and human fibroblast cells in individual genes were calculated using 2-sample *t* tests. The false discovery rate was estimated using the Benjamini and Hochberg method. A false discovery rate cutoff of $\leq$0.05 with a mean fold difference $\geq$2 was used to indicate significance. Functional annotation analysis of differentially expressed genes was performed with the National Institutes of Health Database for Annotation, Visualization and Integrated Discovery (DAVID) web tool (version 6.7, http://david.abcc.ncifcrf.gov/)[10] using Biological Process Gene Ontology (GO) terms and Kyoto Encyclopedia of Genes and Genomes (KEGG) pathways.

Quantitative Real-time Polymerase Chain Reaction

Gene expression was validated using quantitative real-time polymerase chain reaction (qRT-PCR) performed on the ABI 7000 System (Applied Biosystems) using iQ SYBR green supermix (Bio-Rad), according to manufacturer protocols. First-strand cDNA was generated from total RNA using SuperScript II kit (Life Technologies). The resulting cDNA was used as input to each qRT-PCR, along with the appropriate gene-specific primers and PCR reagents. All primers were designed using the Primer-BLAST program from NCBI website. Primer sequences are available upon request. All qRT-PCR assays were done in triplicate. Relative quantity was calculated using the ΔΔCT method with glyceraldehyde 3-phosphate dehydrogenase (GAPDH) as the endogenous control.

In Vitro Cell Viability Assay

YP-MEL and NCM patient cells expanded from tumors were plated into 96-well plates (Grenier Bio One) at a concentration of 5×10^3 cells per well. Increasing concentrations of inhibitors (all purchased from ChemieTek) were added to these wells to a final volume of 200 μL per well, as described previously.[11] Corresponding dilutions of the vehicle dimethyl sulfoxide were used as controls. After 96 hours in culture, cell survival was quantified by Alamar blue assay, according to the manufacturer's protocol. The half maximal inhibitory concentration (IC_{50}) values were calculated for each agent based on individual cytotoxicity plots. Drug combination studies were performed according to the method described by Chou.[12] Briefly, the IC_{25} concentration of the first agent was added to increasing concentrations of the second agent, and cell viability under each experimental condition was measured by Alamar blue assay. The new IC_{50} values corresponding to the combination were then calculated and used to derive combination index (CI) values.

Drug Library Screening

All therapeutic agents used in the screening analysis were synthesized, checked for purity, and provided by Chemietek. The details of the screening were described previously.[11] Every agent was tested against YP-MEL and NCM patient cells at 4 concentrations (0.01, 0.1, 1, and 10 μM) in triplicate. Cell viability was measured with Alamar blue assay.

Immunoblotting

YP-MEL cells were grown to ∼75% confluence in 6-well culture plates (Nunc) and then serum-starved for 16 hours. The cells were then treated with BMS-754807, PP242, or PIK-75. After incubation for 4 hours, one of each duplicate well was treated with 20 ng/mL of IGF-I for 15 minutes. The cells were then washed with ice-cold phosphate-buffered saline and lysed in buffer containing 50 mM Tris, 5 mM EDTA, 0.1% SDS, 1% Triton X-100, 0.5% sodium deoxycholate with phosphatase, and protease inhibitors (Sigma). Protein concentrations of the lysates were quantified by BCA Protein Assay (Pierce). Proteins were then separated on a 10% SDS-PAGE gel and transferred onto nitrocellulose membranes (Bio-Rad). The membranes were blocked for 2 hours at 4°C with 5% skim milk powder in phosphate-buffered saline containing 0.1% Tween-20 (Sigma). The blots were incubated with primary antibodies overnight at 4°C, washed, and probed with appropriate secondary antibodies conjugated to horseradish peroxidase (Sigma), followed by a luminol-based substrate, and developed by exposure to x-ray film (Christie InnoMed).

Results

Morphological and Xenograft Studies on NCM Patients' Tumor Cells

Malignant cells (prepared from the autopsy specimen) were cultured overnight and injected subcutaneously into nude (nu/nu) mice. After allowing sufficient time for tumor growth, the animals were visually examined, and the tumor areas were photographed. These areas formed palpable tumors with pigmentation (Fig. 1A). As a control, ATRT cells were also treated under similar conditions. Although the control animals also developed a palpable mass at the inoculation sites, visible pigmentation was not noted (Fig. 1B). The NCM cells to be further analyzed were derived from tumors after careful excision and preparation for microscopy. Hematoxylin and eosin (H&E) staining of the tumor was first visualized at 10X magnification and showed dense cellular infiltrate in the dermis (Fig. 1C).

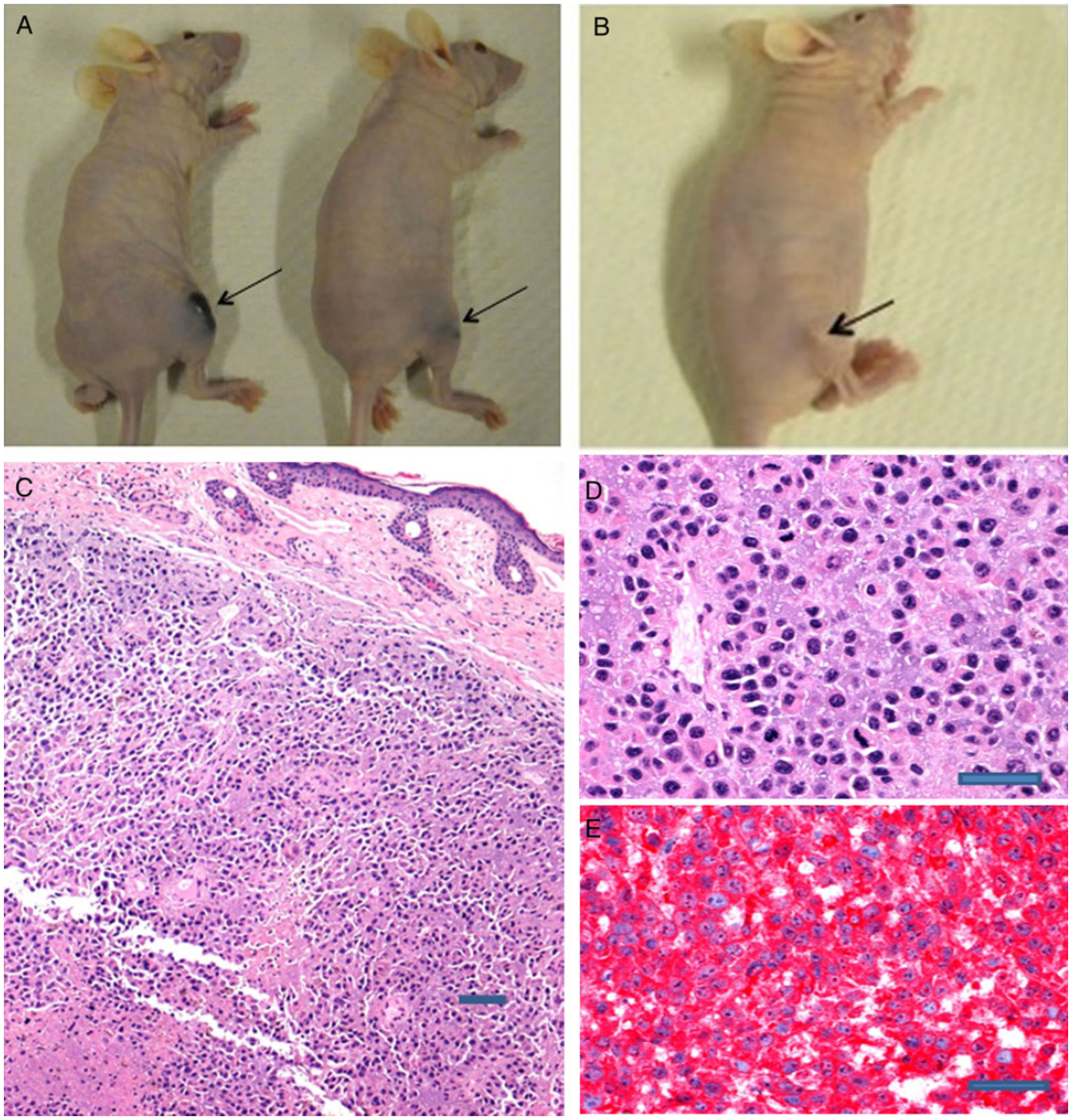

Fig. 1. Establishing NCM xenografts and the characterization of a patient-derived NCM sample. (A). NCM cells that were subcutaneously implanted in nude mice formed tumors that show pigmentation (left, arrows), in comparison with the control (B) nonmelanocytic pediatric brain tumor ATRT cells that yielded nonpigmented tumors. (C) H & E staining of the NCM tumor biopsy from nude mice shows dense cellular infiltrate in the dermis (10X, scale bar is 100 μm) and displays distinct cell morphology. At 40X magnificat ion (scale bars 50 μm), the 2 insets show cells with high nucleo/cytoplasmic ratio and frequent mitoses (D) and diffuse cytoplasmic immunostaining with HMB45 antibody as a marker for melanocytic tumors (E).

Examination under higher magnification showed cells with a high nucleocytoplasmic ratio and frequent mitoses (Fig. 1D). Immunohistochemical analysis with the HMB45 antibody as a marker for melanocytic tumors showed significant immunostaining of these cells (Fig. 1E).

NRAS Mutational Analysis

Next, we wanted to examine the ex vivo patient NCM cells after xenograft for previously described molecular abnormalities. We performed Sanger sequencing on NRAS transcripts to investigate whether NRAS mutation was present in this specimen and in the YP-MEL cell line. Q61K mutation was detected in the YP-MEL cells (Fig. 2A). By contrast, no detectable NRAS mutation was present in the NCM patient cells.

In Vitro Sensitivity to a Panel of MEK Inhibitors

Previous studies have indicated that NRAS mutational status may confer differential sensitivity to MEK inhibition. Therefore, we evaluated the ability of 6 small-molecule MEK inhibitors (all used at 1 μM) using in vitro cytotoxicity assays against YP-MEL and patient NCM cells. Data presented in Fig. 2B illustrate that YP-MEL cells are sensitive to growth inhibition by

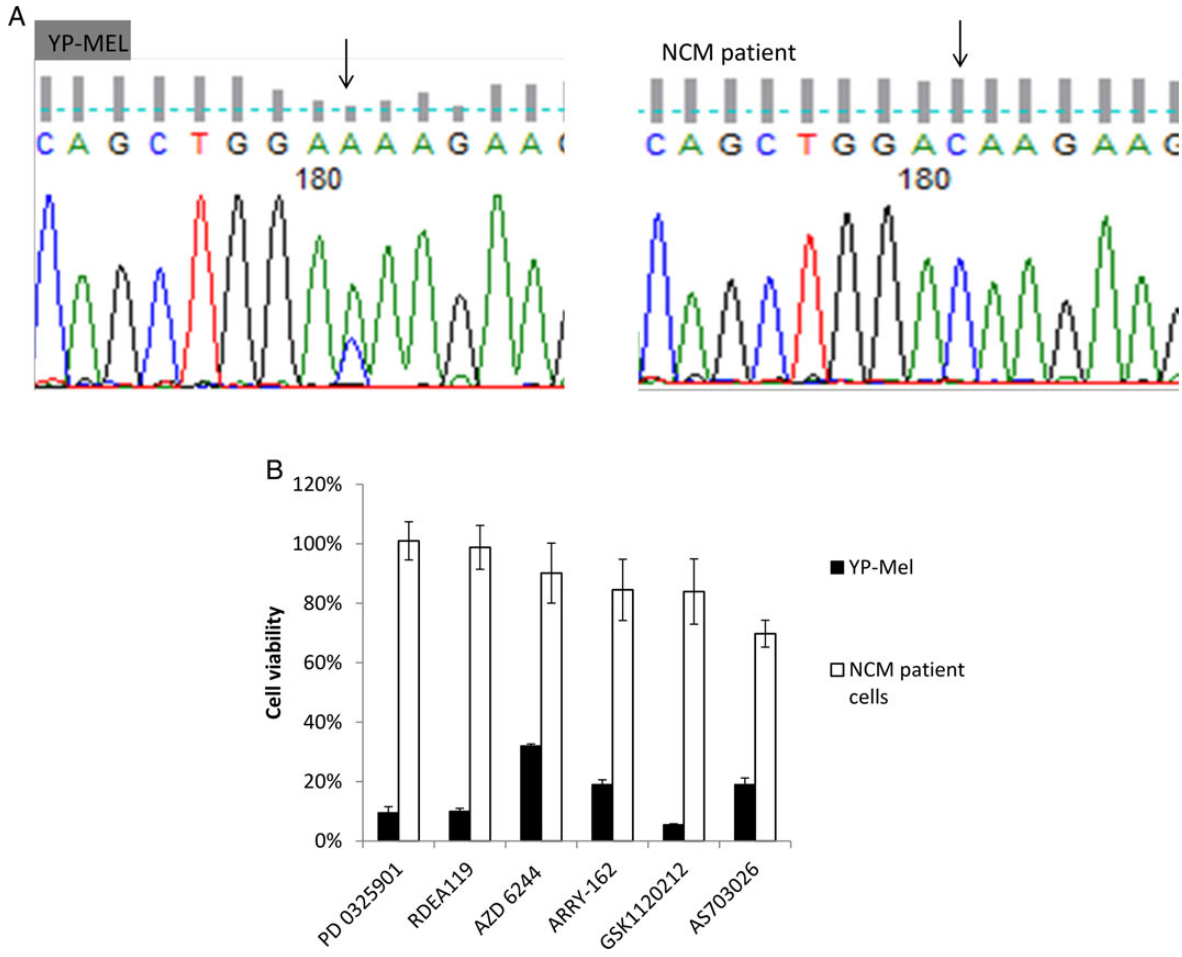

Fig. 2. NRAS mutation correlates with the sensitivity of NCM cells to MEK inhibitors. (A) YP-MEL cell line carries NRAS c. 181C>A (Q61K) mutation, as detected by Sanger sequencing. In contrast, the patient-derived NCM cells do not carry NRAS mutations. (B) The effects of 6 small molecule inhibitors against MEK were evaluated in cytotoxicity assays using YP-MEL and patient NCM cells. Cells were cultured in the presence of the inhibitors at the concentration of 1 μM, and cell viability was measured after 4 days in culture. Here we show growth inhibition in YP-MEL cells compared with NCM patient cells. Data shown are representative of 3 independent experiments.

MEK inhibitors, whereas the patient NCM cells show relative resistance to these agents.

Gene Expression Analysis of YP-MEL and NCM Patient Cells

NCM is considered to be a malignant lesion originating from melanocytic precursors in the brain. However, the difference between NCM and brain metastasis of melanoma has not been reported. In order to identify unique gene expression signatures of NCM, we examined the gene expression profiles of YP-MEL cells, NCM patient cells, WC00090 brain melanoma cells, and normal skin fibroblasts. Although they cannot be considered as perfect reference specimens, normal skin fibroblasts provide a source for rapidly growing yet nonmalignant cells, and the WC00090 cells provide a reference for melanoma cells with CNS metastatic potential.

Data obtained in these analyses showed that 218 genes were differentially expressed in both YP-MEL and NCM patient cells, in contrast to brain melanoma and skin fibroblasts including 61 upregulated and 157 downregulated genes. A list of the top 20 upregulated and downregulated genes is provided in Fig. 3A. (A more comprehensive list of altered genes is included in Supplementary Table S1). To validate the findings of the microarray analyses, we selected 4 genes of interest (DANCR [also known as KIAA0114], IL8, CDKN1A, and IGFBP3) and performed quantitative PCR. After normalization to the GAPDH and gene levels in human fibroblasts, all 4 genes showed consistent fold changes when compared with the microarray data (Fig. 3B).

We then investigated potential biological processes that might have demonstrated enrichment by this gene list. DAVID functional annotation tools were used to identify the GO biological processes or KEGG pathways. Processes that were enriched by upregulated genes in the NCM cells included intracellular organelle lumen, ribosome biogenesis, and RNA processing (P value $< .05$) (Supplementary Table S2). Processes that were enriched by downregulated genes included extracellular matrix, the response to extracellular stimuli, vasculature development, and cell migration (P value $<.005$). It was noteworthy that 4 of the top 50 downregulated genes were involved

A

Top 20 down-regulated genes	Average Fold Change	Top 20 up-regulated genes	Average Fold Change
IGFBP3	-105.3	EEF1A2	33.4
THBS1	-57.4	CKB	14.6
LGALS1	-54.9	GAL	13.4
KIAA1199	-44.5	MIR1974	11.0
PTRF	-44.2	EBP	8.7
SPARC	-39.5	HBQ1	7.3
DCN	-35.1	NPM3	6.4
S100A6	-31.4	PLCXD1	6.0
ANXA1	-30.8	FAM69B	5.9
ANXA2P1	-30.2	SNRPA1	5.3
MT2A	-27.7	LIN28B	5.1
SLC16A3	-26.5	APOA1BP	4.6
ADM	-23.7	COMTD1	4.6
EMP1	-22.6	CCNB1IP1	4.5
IL8	-20.6	MYC	4.4
IGFBP6	-20.3	SLC29A2	4.4
CAV1	-18.5	TUBB4	4.3
LGALS3	-18.2	TRAP1	4.2
CD44	-18.1	RPL29	4.0

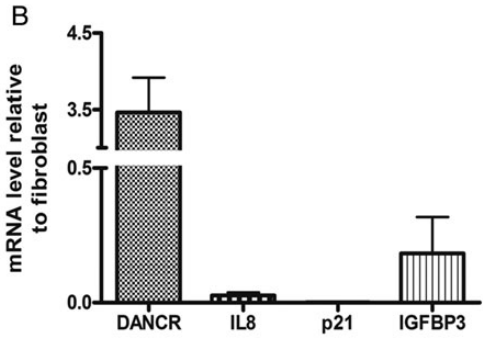

Fig. 3. Gene expression profiling of NCM cell. (A) A list of the top 20 upregulated and downregulated genes in YP-MEL and NCM patient cells according to microarray experiment. (B) qPCR validation of the gene expression analysis. Four genes of interest were selected to perform quantitative PCR. Data are presented as fold changes in the means expression values for each gene after normalization to GAPDH and levels in human fibroblasts.

in the modulation of insulin-like growth factor (IGF) signaling including IGFBP-3, -5, -6 and -7. On the other hand, LIN28B, a microRNA-binding protein that enhances the translation of IGF-2, was present in the upregulated gene list.[13,14] Based on these findings, we explored the potential of IGF pathway components as druggable targets in NCM.

NCM Cells Are Sensitive to IGF-IR and mTOR Pathway Inhibition

We tested 3 IGF-IR inhibitors (BMS-754807, AEW-541, and OSI-906) for in vitro cytotoxicity against YP-MEL and patient NCM cells. Normal human fibroblast cells were used as the control. Both NCM cells showed significant sensitivity to the IGF-IR inhibitors when compared with the human fibroblasts (Fig. 4). In addition, we also examined the effects of inhibiting PI3K and mTOR, which are downstream targets of IGF-IR activity. Both mTORC1/2 inhibitors (rapamycin, PP242, and INK-128) and PI3K inhibitors (PF-04691502, PIK75, and GDC-0980) led to decreased NCM cell proliferation (Fig. 5). Furthermore, we also observed synergy when IGF-IR and PI3K/mTOR inhibitors were used in combination in YP-MEL cells (Fig. 6A). When 1 μM of BMS-754807 was used alone, only a moderate cytotoxic effect was observed (66% of the cells remained alive). However, when combined with a low dose of PP242 or PIK75, which did not induce significant cell death on its own, the cytotoxic effect was significantly stronger than when each inhibitor was used alone. Only a small proportion of the cells survived (16% for PP242 and 33% for PIK75) with the combination treatment. Combination indices calculated using the Chou-Talalay method were both smaller than 1, indicating that the combination was synergistic under this experimental condition.

In order to verify the effects on downstream signaling on IGF-IR inhibition, we treated YP-MEL cells with BMS-754807, a potent and specific IGF-IR/InsR inhibitor. IGF-IR inhibition resulted in blockage of IGF-I-induced IGF-IR activation together with inhibition of phospho-AKT (Ser473), which was detected by Western blot (Fig. 6B). By comparison, the mTORC1/2 inhibitor, PP242, or the PI3K inhibitor, PIK-75, was unable to block IGF-I-induced IGF-IR activation. Interestingly, PP242 completely blocked AKT activation, whereas PIK-75 only partially reduced the level of phospho-AKT, which implicates the potential of an active feedback loop of re-phosphorylating AKT via mTORC2 in YP-MEL cells. Consistent with this, the mTORC1 inhibitor rapamycin was not able to block IGF-I-stimulated AKT activation (data not shown).

Tumor cells, obtained from biopsy specimens that can be established in culture to provide a means of performing in vitro drug-sensitivity assays, enable a practical and efficient experimental approach to identifying targeted therapeutics in precision medicine. To explore the utility of NCM xenograft-derived tumors for facilitating this approach, we examined the activity of agents from a pharmaceutical pipeline library that included clinically feasible small molecule inhibitors against various components of cancer growth and survival pathways. These libraries comprise a total of 150 individual agents. In these experiments, patient NCM cells and YP-MEL cells were treated with increasing dilutions (0.01–10 μM) of each therapeutic agent, and after cell viability under each experimental condition was enumerated by Alamar blue assay after 4 days in culture. From these assays, the corresponding half maximal inhibitory concentration (IC_{50}) values were calculated. (Supplementary Table S3 summarizes the data of agents with IC_{50} values $\leq$1 μM in at least one cell type.) These initial screening data

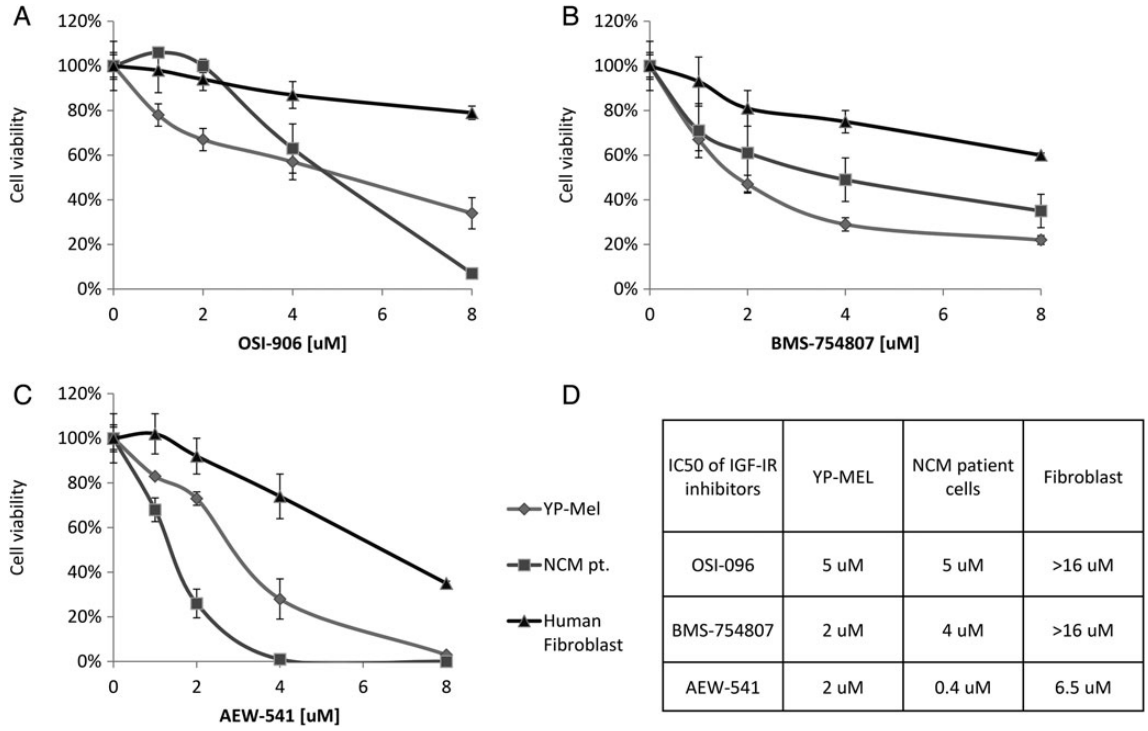

IC50 of IGF-IR inhibitors	YP-MEL	NCM patient cells	Fibroblast
OSI-096	5 uM	5 uM	>16 uM
BMS-754807	2 uM	4 uM	>16 uM
AEW-541	2 uM	0.4 uM	6.5 uM

Fig. 4. NCM cells are sensitive to IGF-IR pathway inhibition. NCM patient cells and human fibroblast cells were tested in a 4-day cytotoxicity assay using 3 different IGF-IR inhibitors (A, OSI-906[μM]; B, BMS-754807[μM]; C, AEW-541[μM])). After treatment with the inhibitors for 4 days, cell viability was measured by Alamar blue assay. IC_{50} values were calculated by plotting cell death in treated cells against dimethyl sulfoxide controls, and these values are given in columns (D).

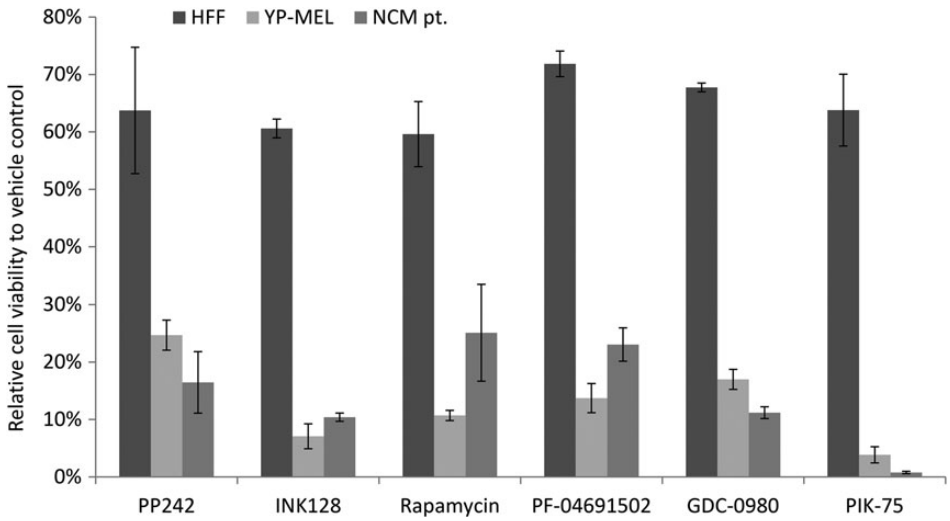

Fig. 5. Effects of targeted inhibitors to PI3K/Akt/mTOR pathway in NCM cell proliferation. YP-MEL and NCM patient cells were treated with increasing concentrations of 6 separate agents as described in Materials and Methods. Normal skin fibroblasts were used as control. Data are presented as relative growth inhibition seen upon treatment with PP242 (4 μM), INK128 (2 μM), rapamycin (10 μM), PF-04691502 (0.5 μM), GDC-0980 (2 μM) and PIK-75 (0.5 μM) compared with dimethyl sulfoxide control for each cell type.

show the differences, as well as the similarities, in activity profiles of selected agents between the 2 cells. As a family of agents, proteasome inhibitors, HSP90 inhibitors, and tubulin stabilizers inhibited both cell lines. Interestingly (consistent with the data presented in Fig. 2), all of the tested MEK inhibitors were significantly active against YP-MEL cells compared with NCM patient cells. The BH3 mimetics ABT-737/ABT-263 also showed better activity against the NCM patient cells.

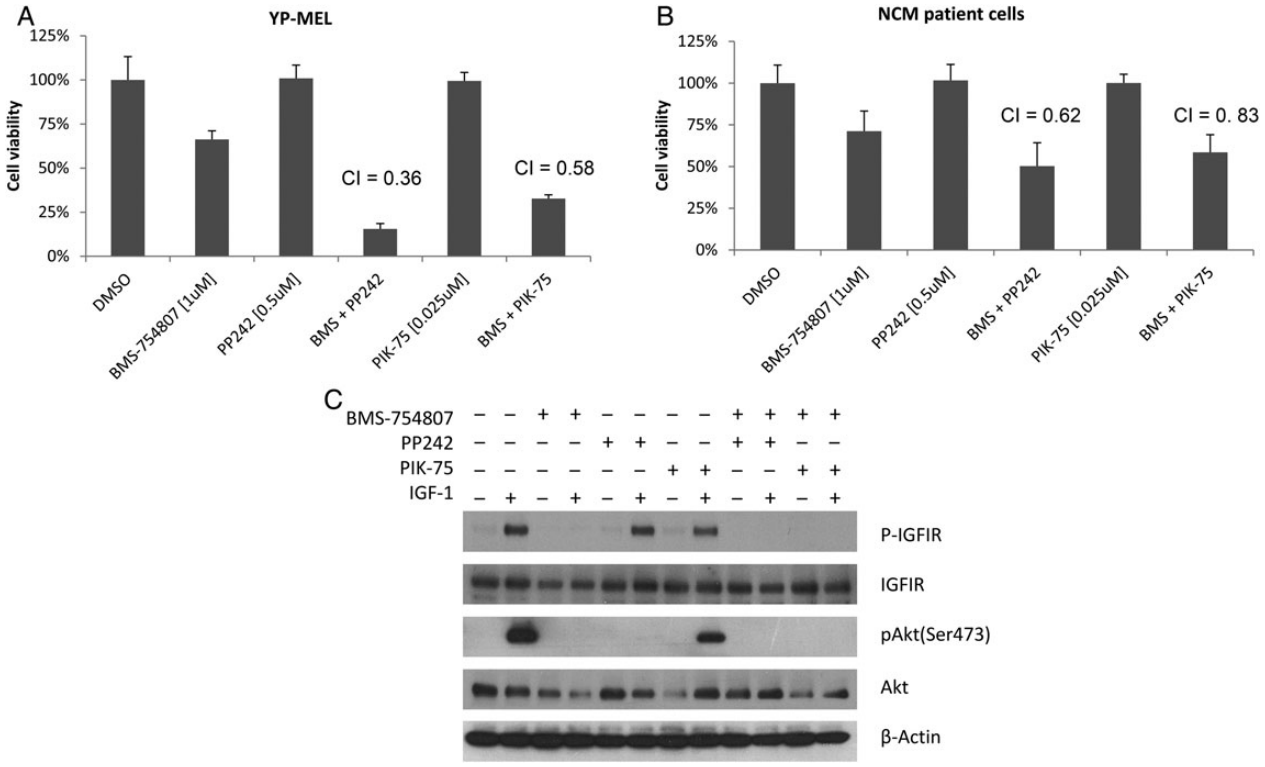

Fig. 6. Combinatorial effect of targeting IGF-IR and PI3K/mTOR pathways in NCM. YP-MEL cells (A) and NCM patient cells (B) were treated with IGF-IR inhibitor BMS-754807, either alone or in combination with mTOR inhibitor PP242 and PI3K inhibitor PIK-75. Combination indices (CI) were calculated using the Chou-Talalay method. CI values <1 indicate that the combinations showed synergy under these experimental conditions. (C) Effect of IGF-IR and PI3K/mTOR inhibition on downstream signaling in YP-MEL cells. Cells were treated with BMS-754807, a specific IGF-IR/InsR inhibitor alone or in combination with themTORC1/2 inhibitor PP242 or the PI3K inhibitor PIK-75. Cell lysates were prepared in the presence of protease and phosphatase inhibitors, and protein levels were evaluated by Western blot analysis using antibodies against total and active IGF-IR and AKT.

Discussion

NCM currently carries an extremely poor prognosis because very little information is available on effective druggable targets for this tumor. In part, this is owing to the rarity of the disease and the lack of well-characterized cell lines and in vitro cell culture platforms required to identify effective targets for therapeutics. In this report, we describe continuously growing NCM cells from a biopsy specimen and their application in subsequent molecular and drug-sensitivity studies.

First, we showed that NCM cells isolated from a biopsy specimen developed tumors in mice with characteristic tissue-specific biological features such as pigment production (Fig. 1). Because these cells represented fresh cells obtained from deposits of leptomeningeal melanocytosis, we also further characterized a parallel cell line that was previously established from an intracranial malignant melanoma in an NCM patient. Our aim was to develop an experimental protocol whereby multiple primary tumor specimens could be analyzed and the inclusion of a stable cell line could serve as a reference source when making comparisons. Recent studies by Kinsler et al showed that oncogenic missense mutations of NRAS codon 61 were present in the tumor tissue of patients with congenital melanocytic nevi.[6] This codon, by virtue of being part of the GTP-binding site, plays a critical role in the normal inactivation process, and mutations at this site lead to constitutive activation of NRAS. Congenital expression of oncogenic NRAS in melanocytes has been shown to drive the primary melanoma of the CNS in children.[15] Previously, preclinical and target modulation studies indicated the potential for activity by MEK inhibitors in NRAS-activated NCM tumors.[16] In our screening, the YP-MEL cells were found to have NRAS codon 61 mutation, which was not detected in our patient cells (Fig. 2A). Accordingly, this defect correlated with in vitro growth inhibition by a panel of MEK inhibitors (Fig. 2B). This observation indicates the need for a focused evaluation of cells and subsequent stratification for treatment with MEK inhibitors in future clinical studies.

As an initial step in investigating the molecular landscape of NCM, expression profiling was carried out to generate a list of genes and cellular pathways that were potentially altered in these cells (Fig. 3). Of these, the molecules that relate IGF-I activity were of particular interest. Previous studies have indicated a role for IGF-I regulated tumor growth and survival pathways in a number of tumors, including melanoma. It has been shown that melanoma cells express the mRNA and secrete IGF-I and, functionally, cell proliferation decreases in response to the antibody blockade of IGF-I.[17] In NCM cells, IGF-I promoted

resistance to apoptosis through increased expression of pro-survival proteins such as BCL2, BCL-X(L) and survivin.[18] It also increased tumor cell migration significantly.[19] The bioavailability of IGF-I for its receptor binding is negatively regulated by IGF-I-binding proteins (IGFBP 1–6), particularly IGFBP-3. Interestingly, the gene expression profile of NCM cells showed that *IGFBP-3, -6*, and *-7* were among the most downregulated genes in our analysis. It has been suggested that a reduction of serum IGFBP-3 levels and the associated increased availability of IGFs may represent active growth and metastatic mechanisms in melanoma.[20] This has indicated that there are grounds to further explore the effects of IGF-I inhibition, specifically in NCM cells. Similar to the findings in melanoma, the NCM cells also showed growth inhibition when exposed to IGF-I-targeted agents (Fig. 4), which suggests that there is a role for such therapeutic approaches, as a single agent or in combination, in the treatment of NCM.

Our gene expression analysis also indicated the potential involvement of other relevant pathways in NCM cells. For example, we noted significant downregulation of the angiogenesis inhibitor THBS1. An important role by this molecule has already been demonstrated in tumor cell growth, adhesion, migration, angiogenesis, and tumor metastasis,.[21] Mechanistically, promoter hypermethylation has been shown to be a potential process for decreased expression of this gene in melanoma compared with nonmalignant nevi.[22] Gene expression profiling studies have also demonstrated the downregulation of the *GAL-1* gene. Secreted or extracellular GAL-1 has been shown to promote angiogenesis and tumor growth as well as immune dysregulation. However, a complex relationship appears to exist between intracellular GAL-1 and tumor cell survival. For example, *GAL-1* expression is epigenetically regulated through promoter hypermethylation in the colorectal cancer model, which enables tumor cell proliferation and escape of apoptosis.[23] Conversely, we also noted a number of genes with oncogenic potential that were upregulated in the NCM cells. For example, the *EEF1A2* gene, when expressed in an *EEF1A2*-negative ovarian cell line, showed more tumorigenic properties than its parental control, suggesting its potential as a putative oncogene.[24] Overall, initial gene expression data support the feasibility of using cells from an expanded cohort of patients in future studies to identify potential druggable targets and cell growth regulatory pathways in NCM.

Although, targeted inhibition of IGF-IR will be explored in future treatment modalities, effective drug combinations must be investigated to overcome the potential for treatment resistance in vivo. Based on the previously demonstrated ability of IGF-IR signaling to cross talk with other receptor tyrosine kinases, targeting downstream effectors of the IGF-IR pathway may provide the dual benefit of direct, as well as receptor, cross talk inhibition. In addition, it has been suggested that the compensatory activation of associated signaling pathways is a critical mechanism for inducing resistance to IGFR inhibitors. Thus, combining agents that target multiple components in a signaling pathway, in a vertical blockade, can be tested in preclinical models. In our study, synergistic activity was demonstrated when IGF-IR inhibition was combined with agents that block PI3K and mTOR activities in the vertical axis of the IGF-IR-PI3K-AKT-mTOR pathway (Fig. 5 and 6). We also showed that the drug combinations resulted in effective inhibition of the signaling axis, as shown by the blockade of AKT activation in response to IGF-I.

The integration of drug-sensitivity profiles of primary cell cultures with mutational analysis and genomic signatures provides a powerful approach to predicting and cross-validating treatment avenues for precision medicine. We explored the utility of xenograft-expanded NCM cells with in vitro drug screens in the next set of experiments to identify agents that induced potent cell growth inhibition (Supplementary Table S3). Our findings showed that, as functional groups, the proteasome inhibitors and HSP inhibitors demonstrated significant activity against both NCM cells. This is in agreement with a study that evaluated human cutaneous melanoma-derived cell lines, in which significant growth inhibition by a panel of proteasome inhibitors was reported.[25] Furthermore, this activity was found to be mediated by caspase-dependent and caspase-independent mechanisms. Similarly, the effect of HSP90 inhibition has been evaluated in a number of tumors, including melanoma-derived cells.[26] For example, in a recent study, the HSP90 inhibitor ganetespib showed significant antiproliferative activity against cutaneous melanoma cells, including those with BRAF and NRAS mutations as well as those with acquired resistance to B-RAF inhibitors.[27] However, The YP-MEL cell line exhibited significantly more sensitivity to MEK and PI3K inhibitors. Overall, YP-MEL showed higher sensitivity to more agents than the cultured NCM cells, consistent with their closer resemblance to primary tumor cells.[17]

In summary, our study demonstrated that, as a proof of concept, cells taken from NCM biopsy specimens can be successfully expanded in xenografts to provide material to interrogate the functional molecular and drug-sensitivity properties. Furthermore, we provided evidence that these cells utilize the IGF-IR pathway, which can be effectively blocked by interference with multiple components in the vertical axis of its signal transduction machinery. We also identified, using in vitro sensitivity drug screens, that a number of targeted therapeutic agents may hold promise for future clinical applications. Based on these data, additional studies should be carried out using an expanded number of NCM specimens to establish applicable information regarding the biology and future effective treatment modalities for NCM.

Supplementary Material

Supplementary material is available online at *Neuro-Oncology* (http://neuro-oncology.oxfordjournals.org/).

Funding

This study was supported in part by grants from the Alberta Children's Hospital Foundation, Kids Cancer Care Foundation of Alberta (KCCFA), and the POETIC Foundation.

Acknowledgments

We acknowledge the support of Nevus Outreach. We also acknowledge the technical assistance provided by Dr. Kimberley Hoeksema.

Conflict of interest statement. Authors declare no conflict of interest.

References

1. Kadonaga JN, Frieden IJ. Neurocutaneous melanosis: definition and review of the literature. *J Am Acad Dermatol*. 1991;(5 Pt 1):24:747–755.
2. Shah KN. The risk of melanoma and neurocutaneous melanosis associated with congenital melanocytic nevi. *Semin Cutan Med Surg*. 2010;29(3):159–164.
3. Agero AL, Benvenuto-Andrade C, Dusza SW, et al. Asymptomatic neurocutaneous melanocytosis in patients with large congenital melanocytic nevi: a study of cases from an Internet-based registry. *J Am Acad Dermatol*. 2005;53(6):959–965.
4. Arneja JS, Gosain AK. Giant congenital melanocytic nevi. *Plast Reconstr Surg*. 2009;124(1 Suppl):1e–13e.
5. Cramer SF. The melanocytic differentiation pathway in congenital melanocytic nevi: theoretical considerations. *Pediatr Pathol*. 1988; 8(3):253–265.
6. Kinsler VA, Thomas AC, Ishida M, et al. Multiple congenital melanocytic nevi and neurocutaneous melanosis are caused by postzygotic mutations in codon 61 of NRAS. *J Invest Dermatol*. 2013;133(9):2229–2236.
7. Ball NJ, Yohn JJ, Morelli JG, et al. Ras mutations in human melanoma: a marker of malignant progression. *J Invest Dermatol*. 1994;102(3):285–290.
8. Charbel C, Fontaine RH, Malouf GG, et al. NRAS mutation is the sole recurrent somatic mutation in large congenital melanocytic nevi. *J Invest Dermatol*. 2014;134(4):1067–1074.
9. Nagashima Y, Miyagi Y, Aoki I, et al. Establishment and characterization of a malignant melanoma cell line (YP-MEL) derived from a patient with neurocutaneous melanosis. *Pathol Res Pract*. 1994;190(2):178–185.
10. Huang da W, Sherman BT, Lempicki RA. Systematic and integrative analysis of large gene lists using DAVID bioinformatics resources. *Nat Protoc*. 2009;4(1):44–57.
11. Singh A, Lun X, Jayanthan A, et al. Profiling pathway-specific novel therapeutics in preclinical assessment for central nervous system atypical teratoid rhabdoid tumors (CNS ATRT): favorable activity of targeting. *Mol Oncol*. 2013;7(3):497–512.
12. Chou TC. Drug combination studies and their synergy quantification using the Chou-Talalay method. *Cancer Res*. 2010; 70(2):440–446.
13. Alajez NM, Shi W, Wong D, et al. Lin28b promotes head and neck cancer progression via modulation of the insulin-like growth factor survival pathway. *Oncotarget*. 2012;3(12):1641–1652.
14. Polesskaya A, Cuvellier S, Naguibneva I, et al. Lin-28 binds IGF-2 mRNA and participates in skeletal myogenesis by increasing translation efficiency. *Genes Dev*. 2007;21(9):1125–1138.
15. Pedersen M, Kusters-Vandevelde HV, Viros A, et al. Primary melanoma of the CNS in children is driven by congenital expression of oncogenic NRAS in melanocytes. *Cancer Discov*. 2013;3(4):458–469.
16. Kusters-Vandevelde HV, Willemsen AE, Groenen PJ, et al. Experimental treatment of NRAS-mutated neurocutaneous melanocytosis with MEK162, a MEK-inhibitor. *Acta Neuropathol Commun*. 2014;2:41.
17. Molhoek KR, Shada AL, Smolkin M, et al. Comprehensive analysis of receptor tyrosine kinase activation in human melanomas reveals autocrine signaling through IGF-1R. *Melanoma Res*. 2011;21(4): 274–284.
18. Hilmi C, Larribere L, Giuliano S, et al. IGF1 promotes resistance to apoptosis in melanoma cells through an increased expression of BCL2, BCL-X(L), and survivin. *J Invest Dermatol*. 2008;128(6): 1499–1505.
19. Neudauer CL, McCarthy JB. Insulin-like growth factor I-stimulated melanoma cell migration requires phosphoinositide 3-kinase but not extracellular-regulated kinase activation. *Exp Cell Res*. 2003; 286(1):128–137.
20. Grimberg A, Cohen P. Role of insulin-like growth factors and their binding proteins in growth control and carcinogenesis. *J Cell Physiol*. 2000;183(1):1–9.
21. Kazerounian S, Yee KO, Lawler J. Thrombospondins in cancer. *Cell Mol Life Sci*. 2008;65(5):700–712.
22. Lindner DJ, Wu Y, Haney R, et al. Thrombospondin-1 expression in melanoma is blocked by methylation and targeted reversal by 5-Aza-deoxycytidine suppresses angiogenesis. *Matrix Biol*. 2013; 32(2):123–132.
23. Satelli A, Rao US. Galectin-1 is silenced by promoter hypermethylation and its re-expression induces apoptosis in human colorectal cancer cells. *Cancer Lett*. 2011;301(1):38–46.
24. Anand N, Murthy S, Amann G, et al. Protein elongation factor EEF1A2 is a putative oncogene in ovarian cancer. *Nat Genet*. 2002;31(3):301–305.
25. Sorolla A, Yeramian A, Dolcet X, et al. Effect of proteasome inhibitors on proliferation and apoptosis of human cutaneous melanoma-derived cell lines. *Br J Dermatol*. 2008;158(3): 496–504.
26. Giménez Ortiz A, Montalar Salcedo J. Heat shock proteins as targets in oncology. *Clin Transl Oncol*. 2010;12(3):166–173.
27. Wu X, Marmarelis ME, Hodi FS. Activity of the heat shock protein 90 inhibitor ganetespib in melanoma. *PLoS One*. 2013; 8(2):e56134.